Time-lapse tracking of barley androgenesis reveals position-determined cell death within pro-embryos

Maraschin, S. de F.; Vennik M.; Lamers, G.E.M.; Spaink, H.P.; Wang, M.

Planta (2005) 220: 531–540
DOI 10.1007/s00425-004-1371-x

ORIGINAL ARTICLE

Simone de F. Maraschin · Marco Vennik
Gerda E. M. Lamers · Herman P. Spaink · Mei Wang

Time-lapse tracking of barley androgenesis reveals position-determined cell death within pro-embryos

Received: 5 March 2004 / Accepted: 20 July 2004 / Published online: 24 September 2004

Abstract Following abiotic stress to induce barley (*Hordeum vulgare* L.) androgenesis, the development of 794 enlarged microspores in culture was monitored by time-lapse tracking. In total, 11% of the microspores tracked developed into embryo-like structures (type-I pathway), 36% formed multicellular structures (type-II pathway) and 53% of the microspores followed gametophytic divisions, accumulated starch and died in the first days of tracking (type-III pathway). Despite the microspore fate, enlarged microspores showed similar morphologies directly after stress treatment. Ultrastructural analysis, however, revealed two morphologically distinct cell types. Cells with a thin intine layer and an undifferentiated cytoplasm after stress treatment were associated with type-I and type-II pathways, whereas the presence of differentiated amyloplasts and a thick intine layer were associated with the type-III pathway. Tracking revealed that the first morphological change associated with embryogenic potential was a star-like morphology, which was a transitory stage between uninucleate vacuolated microspores after stress and the initiation of cell division. The difference between type-I and type-II pathways was observed during the time they displayed the star-like morphology. During the transition phase, embryo-like structures in the type-I pathway were always released out of the exine wall at the opposite side of the pollen germ pore, whereas in the type-II pathway multicellular structures were unable to break the exine and to release embryo-like structures. Moreover, by combining viability studies with cell tracking, we show that release of embryo-like structures was preceded by a decrease in viability of the cells positioned at the site of exine wall rupture. These cells were also positively stained by Sytox orange, a cell death indicator. Thereby, we demonstrate, for the first time, that a position-determined cell death process marks the transition from a multicellular structure into an embryo-like structure during barley androgenesis.

Keywords Androgenesis · Cell death · *Hordeum* · Microspore embryogenesis · Time-lapse tracking

Abbreviations CLSM: Confocal laser scanning microscopy · ELS: Embryo-like structure released out of the exine wall · FDA: Fluorescein diacetate · MCS: Multicellular structure inside the exine wall · TEM: Transmission electron microscopy

S. de F. Maraschin (✉) · M. Vennik · M. Wang
Center for Phytotechnology LU/TNO,
Leiden University, Wassenaarseweg 64, 2333 AL Leiden,
The Netherlands
E-mail: maraschin@rulbim.leidenuniv.nl
Tel.: +31-71-5274909
Fax: +31-71-5274999

M. Vennik · M. Wang
TNO Department of Applied Plant Sciences,
Zernikedreef 9, P.O. Box 2215, 2301 CE Leiden,
The Netherlands

G. E. M. Lamers · H. P. Spaink
Institute of Biology Leiden, Leiden University,
Wassenaarseweg 64, P.O. Box 9505, 2300 RA Leiden,
The Netherlands

Introduction

During androgenesis, haploid microspores initially determined to form gametes are reprogrammed to divide and to form embryos, which develop similarly to their somatic and zygotic counterparts (Mordhorst et al. 1997). As a result of frequent chromosome doubling, microspore-derived embryos develop into double-haploid plants, providing advantages for both fundamental and applied research (Wang et al. 2000).

Since it was first described in in vitro-cultured anthers of *Datura innoxia* by Guha and Maheshwari (1964), improvement of the conditions for androgenesis induction and microspore culture have resulted in the regeneration of double-haploids of many plant species (Reynolds 1997). Due to the high regeneration

efficiencies, rapeseed (*Brassica napus* L.), tobacco (*Nicotiana* ssp.), wheat (*Triticum aestivum* L.) and barley (*Hordeum vulgare* L.) are considered model systems for androgenesis studies (Touraev et al. 1997). These species offer the possibility for the identification of the genes involved in androgenesis induction and for the development of molecular markers. However, only a few marker genes have been identified so far. Among these, members of the family of heat-shock proteins, napin seed storage proteins and the *BABY BOOM* gene have been shown to correlate with *Brassica* androgenesis initiation (Smykal and Pechan 2000; Boutilier et al. 1994, 2002).

One of the most pertinent problems in the search for suitable molecular markers for microspore embryogenic competence is the heterogeneity of stressed microspore populations, which are composed of embryogenic and non-embryogenic cells (Pechan and Smykal 2001). Therefore, the identification and isolation of the competent microspores following stress treatment is of great importance. Time-lapse tracking offers the possibility to follow the developmental pathway from single cells to embryos in detail (Krens et al. 1998). This technique has been employed in the identification of morphological traits for the induction of embryogenesis in many plant cell cultures, such as barley and tobacco protoplasts, single suspension cells of carrot (*Daucus carota* L.), leaf explants from *Dactylis glomerata* L. and pro-embryogenic masses of Norway spruce (*Picea abies* L. Karst) (Golds et al. 1992; Toonen et al. 1994; Somleva et al. 2000; Filonova et al. 2000a). The identification of cells competent to form embryos in carrot somatic embryogenesis has helped the development of robust embryogenic marker genes, such as the *Somatic embryogenesis receptor-like Kinase* (*SERK*) and the *EP2* gene, which encodes a lipid-transfer protein (Schmidt et al. 1997; Sterk et al. 1991).

In the field of androgenesis, an efficient system of tracking heat-stressed wheat microspores to the embryo stage has been developed by Indrianto et al. (2001), whose findings indicate that a star-like morphology is correlated with embryogenic competence. Single-cell tracking of barley microspores following cold or heat stress to induce androgenesis revealed that only enlarged microspores with a rich cytoplasm and granular appearance were able to develop into embryos (Bolik and Koop 1991; Kumlehn and Lörz 1999). So far, the highest regeneration efficiencies from barley microspores have been obtained by the incubation of anthers containing uninucleate microspores in mannitol solution for 4 days at 25°C. After stress treatment, an average of 20–60% of the microspores appear as enlarged, highly vacuolated cells, an indication of embryogenic potential acquirement (Hoekstra et al. 1992). However, only 7% of these enlarged microspores have been reported to develop into embryo-like structures (Maraschin et al. 2003). In order to gain more information on the morphology of the enlarged cells that ultimately contribute to embryo formation during barley androgenesis following mannitol starvation treatment, ultrastructural studies and time-lapse tracking of isolated enlarged microspores immobilized in a thin layer of agarose were carried out. Time-lapse tracking was coupled to viability studies, and the successive developmental stages from single barley microspores to embryos were determined, resulting in the elaboration of a fate map of barley microspore embryogenesis. We demonstrate that the star-like morphology indicates a developmental process, and its time of occurrence is associated with the embryogenic potential of barley microspores. Moreover, we report, for the first time, that the transition from a multicellular structure to an embryo-like structure is accompanied by cell death.

Materials and methods

Androgenesis induction, microspore culture and time-lapse tracking

Donor plants of barley (*Hordeum vulgare* L. cv. Igri; Landbouw Bureau Wiersum, The Netherlands) were grown in a phytotron under conditions described previously (Hoekstra et al. 1992). Pre-treatment consisted of incubation of anthers containing mid-late to late uninucleate microspores in 0.37 M mannitol solution for 4 days in the dark, at 25°C (Hoekstra et al. 1992). After pre-treatment, microspores were isolated by gentle blending in 0.37 M mannitol solution for 30 s using a commercial blender at medium power (Waring), filtered through 110-μm nylon meshes and collected by centrifugation at 800 rpm for 5 min. The number of enlarged and non-enlarged microspores was estimated in a population of 300 cells in three independent experiments ($n=3$). The enlarged microspores were separated from the non-enlarged ones by a sucrose gradient (Maraschin et al. 2003). The enlarged microspores were plated in medium I (Hoekstra et al. 1992) at a density of 2×10^4 enlarged microspores per ml, and cultured for 7 days (Hoekstra et al. 1993) for viability studies of multicellular structures (MCSs) or immobilized for time-lapse tracking. Microspores were immobilized onto sterilized 500-μm nylon meshes in 8-well Lab-Tek II chambers (Nalge Nunc International). For immobilization, each well held 200 μl of medium I (Hoekstra et al. 1992) containing 0.6% (w/v) of low-melting-type agarose (Hispanagar) and 2×10^4 enlarged microspores per ml. The thin layer of immobilized microspores was covered by 500 μl of medium I per well (Hoekstra et al. 1992) and the cultures were incubated at 25°C in the dark for 28 days for embryo development. After 1 week of culture, 250 μl of fresh medium I (Hoekstra et al. 1992) was added to each well. Fluorescein diacetate (FDA; Sigma) was used to assay MCS viability during cell tracking. FDA was used at a final concentration of 1×10^{-4} μg ml^{-1} and was added at day 0 of tracked cultures. The development of 794 enlarged microspores was followed in three independent experiments ($n=3$). The immobilized microspores were observed using an

inverted Olympus microscope coupled to a Nikon DXM 1200 digital camera. The position of each microspore was determined using the nylon mesh as a reference guide. Digital images were generated at days 0, 1, 2, 3, 4, 6, 8, 10, 14, 16 and 28 of culture using both light and fluorescence microscopy. The microspores were characterized into different types according to their developmental pathways. After 28 days of culture, embryos ranging from 0.5 to 1 mm were transferred to regeneration medium (Hoekstra et al. 1992).

Transmission electron microscopy

Enlarged microspores after stress treatment were assayed for ultrastructural studies. Microspores were fixed in a mixture of 2% (w/v) glutaraldehyde and 2.5% (w/v) paraformaldehyde in 0.1 M sodium cacodylate buffer (pH 7.3) for 3 h at room temperature. Microspores were immobilized in 1% (w/v) low-melting-type agarose (Hispanagar) and the resulting pellets were returned to fixative solution overnight at 4°C. Pellets were washed for 10 min in 0.1 M sodium cacodylate buffer (pH 7.3) and placed in 1% (w/v) OsO_4 in 0.1 M sodium cacodylate buffer (pH 7.3) for 1 h at room temperature. Following post-fixation, pellets were washed for 10 min in 0.1 M sodium cacodylate buffer (pH 7.3) and dehydrated at room temperature through a graded ethanol series as follows: 70%, 80%, 90%, 96%, 100% (v/v). After dehydration, pellets were placed in propylene oxide for 30 min. The resin was infiltrated by incubation in a 1:1 (v/v) mixture of propylene oxide:Epon (Agar Scientific) for 2 h, followed by incubation in Epon overnight at room temperature. Embedding was in Epon and polymerization took place at 55°C for 48 h. Ultrathin sections were cut using an ultramicrotome (Ultracut, Leica), stained for 10 min in 2% (w/v) uranyl acetate in 50% (v/v) ethanol and for 10 min in 0.4% (w/v) lead citrate, followed by thorough washes in deionized filtered water. Sections were observed using a Jeol 100 CX electron microscope. Electron micrographs were taken at 60 kV on Kodak 5302 FGP-film.

Cell viability and cell death staining of MCSs

MCSs at day 7 of liquid cultures were stained for cell death with 1 μM Sytox orange (Molecular Probes) and for cell viability with 4×10^{-2} μg ml^{-1} FDA. MCSs were observed using a Leica DM IRBE confocal microscope. Argon and krypton lasers, respectively, were used for visualization of FDA and Sytox orange signals.

Experimental data

Mean values ± SD of the different developmental pathways were calculated as percentages of the relative frequency of each pathway identified. Significance of the differences in mean values was tested using the Student's *t*-test.

Results

Stress-induced developmental pathways identified by time-lapse tracking

Following mannitol and starvation stress, 51.6 ± 4.8% ($n = 3$) of the isolated microspores were composed of enlarged, vacuolated cells with yellow/red interference of the exine wall. These enlarged cells were cultured in a thin layer of agarose for development of embryo-like structures (ELSs). The fate of 794 enlarged cells was followed by time-lapse tracking in three independent experiments ($n = 3$). Developmental stages were observed at different time-points and the microspores were characterized according to their developmental pathways. This system yielded 10.9 ± 4.2% ELSs released out of the exine wall. These ELSs were capable of regenerating into a new plantlet when transferred to germination medium (data not shown). When enlarged microspores are cultured at the same density in liquid medium, 7% of the microspores develop into ELSs (Maraschin et al. 2003). This suggests that the immobilized cultures are comparable to the liquid system.

Mainly three types of developmental pathway were identified (Fig. 1). Developmental type I, or the embryogenic pathway, represented 10.9 ± 4.2% of the microspores tracked. This group comprised the microspores that followed sporophytic cell divisions, formed multicellular structures (MCSs) and were capable of releasing ELSs out of the exine wall of microspores (Fig. 1a–f). MCSs ruptured the exine wall of microspores after 10.5 ± 1.1 days of cell tracking (Fig. 1e). In the liquid culture system, MCSs usually rupture the exine wall of microspores after 7–8 days of culture (van Bergen et al. 1999), thus immobilized cultures display a 2- to 3-day delay compared to liquid ones. Developmental type II (36.2 ± 2.4%) was also represented by microspores that followed sporophytic cell divisions, formed MCSs but showed shrinkage of the whole structure and died in an asynchronous way. Death occurred mostly between days 7 and 10 of culture, prior to the time of exine wall rupture in the type-I developmental pathway (Fig. 1g–k). Eventually, dead material was extruded from the exine wall of these MCSs (Fig. 1k). Microspores grouped into developmental type III (52.9 ± 4.5%) did not display sporophytic divisions and died soon after initiation of culture (Fig. 1l–o).

In order to identify the morphological characteristics of embryogenic microspores at an early developmental stage, microspore morphology at day 0 of tracking from type-I, -II and -III developmental pathways was analyzed. Cells were characterized by the presence of a big central vacuole, surrounded by a narrow strip of cytoplasm in which one nucleus was present. Differences were observed in the nuclear position relative to the pore (0–

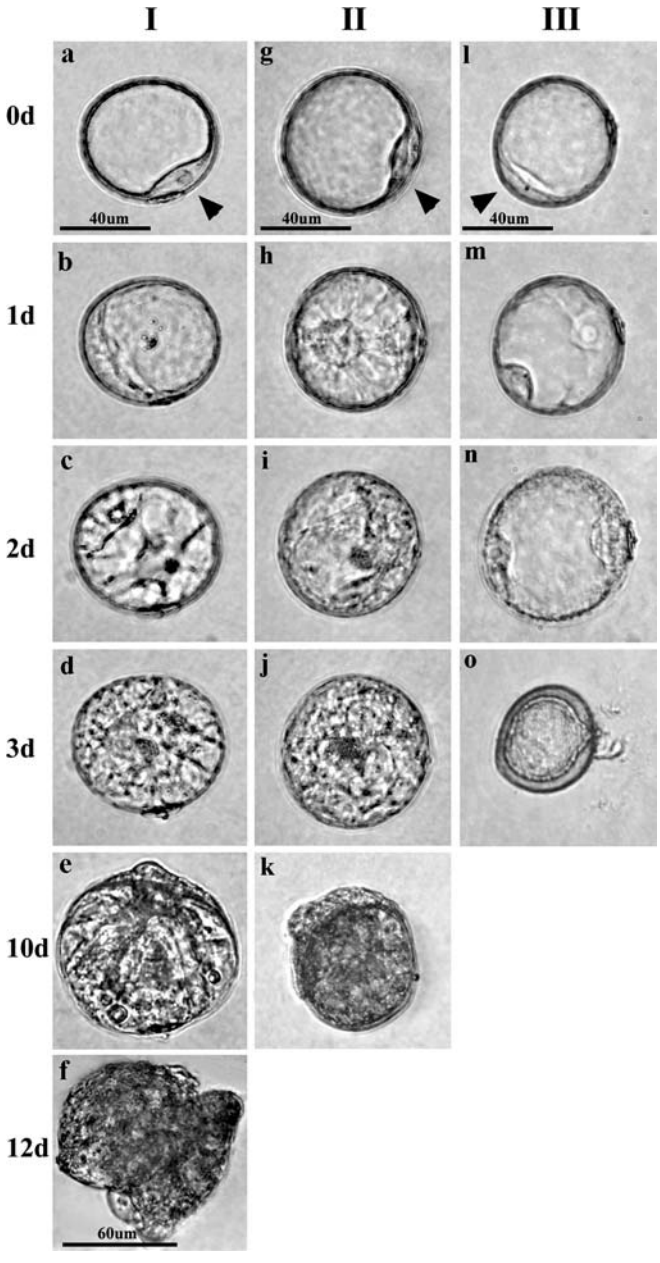

Fig. 1a–o Developmental pathways of stressed enlarged barley (*Hordeum vulgare*) microspores in culture, as determined by time-lapse tracking. According to their type of development, microspores were grouped into type I (**a–f**); type II (**g–k**) and type III (**l–o**). *Arrowheads* in **a**, **g** and **l** indicate the position of the nucleus in relation to the pollen germ pore: 0°, 0° and 90–180°, respectively. Each developmental type is summarized in Table 1

180°), the exine wall light interference (yellow to red) and in the cytoplasm granularity (Fig. 1a,g,l). However, none of these traits was exclusive to any of the developmental types identified. The first morphological change associated with sporophytic development was nuclear migration towards the middle of the microspore. This phenomenon was observed between days 0 and 3 of tracking in 60% of the microspores following developmental types I and II (Fig. 1a–c, g,h). Central localization of the nucleus was observed concomitantly with fragmentation of the large central vacuole, which was interspersed with centripetally oriented cytoplasmic strands. In both developmental types, the acquisition of a star-like morphology of the cells was always followed by sporophytic divisions. By monitoring the evolution of the star-like morphology over a period of 24 h, it was possible to observe that sporophytic divisions commenced characteristically at the side opposite to the pollen germ pore (Fig. 2a–e). In the first 2 h, the centrally located nucleus migrated towards the side opposite to the pollen germ pore (Fig. 2a–c), followed by nuclear division after 4 h (Fig. 2d). After 24 h, more than half of the space contained by the exine was filled by three visible nuclei (Fig. 2e). However, there seemed to be a difference in the time of appearance of the star-like morphology between developmental types I and II (Fig. 1c,h; Table 1). In developmental type II, $85.4 \pm 2.5\%$ of the microspores displayed the star-like morphology in the first 24 h of tracking, whereas only $65.4 \pm 4.8\%$ of the microspores following the type-I pathway showed the star-like morphology in the same period ($P < 0.06$). Microspores following developmental type III were never found to display the star-like morphology. In most cases, microspores displayed gametophytic divisions and died soon after initiation of tracking, indicating that these microspores were still committed to the pollen developmental pathway (Fig. 1l–o). A comparison of developmental types I, II and III is shown in Table 1.

Subcellular differences in enlarged microspores after stress treatment

At day 0 of tracking, irrespective of their developmental pathway, enlarged microspores showed similar morphologies at the light-microscopy level (Fig. 1a,g,l). Ultrastructural studies of enlarged cells at day 0 of culture were carried out using transmission electron microscopy (TEM). Based on their cytological characteristics, mainly two types of enlarged microspore could be identified. One type of microspore showed a large nucleus close to the exine wall and a narrow strip of cytoplasm surrounding the vacuole. The intine was present as a thin layer immediately underneath the exine wall (Fig. 3a–c). In another type of vacuolated microspore with the nucleus close to the exine wall, an organelle-rich cytoplasm, filled with differentiated amyloplasts, and a thick intine layer were present (Fig. 3d–f). Amyloplasts containing starch granules were often associated with microspores with a thick intine layer (Fig. 3d–f), but were never found in microspores that had a thin intine layer (Fig. 3a–c). In the latter, only a few organelles were present, such as rough endoplasmic reticulum, mitochondria and undifferentiated proplastids (Fig. 3b,c). When mid-late to late uninucleate microspores were allowed to further develop in the mother plant for 4 days, they displayed gametophytic cell divisions and developed into binucleate pollen. TEM analysis of these binucleate pollen grains following normal

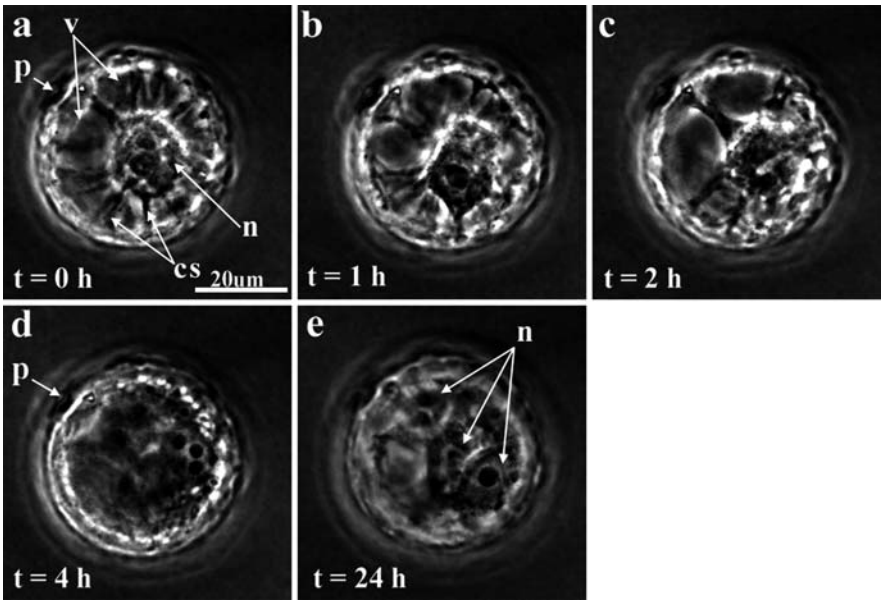

Fig. 2a–e Evolution of a star-like morphology in developmental type I barley microspores, as monitored over a period of 24 h. The star-like morphology was observed from 1 to 2 days of culture by phase contrast. Images were taken every hour from several star-like structures, and representative examples are shown. *cs* Cytoplasmic strands, *n* nucleus, *p* germ pore, *v* vacuole

gametophytic development revealed that these cells possess a thick intine layer and an organelle-rich cytoplasm (Fig. 3g–i). The cytoplasm contained numerous mitochondria, Golgi apparatus, rough and smooth endoplasmic reticulum and starch granules in the differentiated amyloplasts (Fig. 3h,i). This cytoplasmic morphology was similar to that observed in the type of enlarged cell with a thick intine layer, indicating that, morphologically, the latter showed signs of gametophytic development (Fig. 3d–f), which, however, was less advanced than for binucleate pollen, as starch granules were much smaller and less numerous.

Cell viability of developmental type-I and type-II MCSs

Both developmental types I and II gave rise to MCSs and together accounted for 47.1 ± 4.5% of the tracked microspores, in an estimated ratio of 1:5 (I:II). However, microspores following developmental type II never released ELSs out of the exine wall of microspores, indicating that this is a crucial step in the androgenic process of barley. In order to gain more information on the fate of MCSs following developmental types I and II, viability studies were coupled to time-lapse tracking. To do so, FDA was added to the immobilized cultures and observed until the time of exine wall rupture. The FDA concentration used during tracking did not affect the growth rate or the morphology of the cells, suggesting that this FDA concentration is not toxic for microspore-derived embryo development (data not shown). Figure 4 shows representative examples of developmental type I (Fig. 4a–m) and type II (Fig. 4n–y) observed by bright-field and fluorescence microscopy. During the first sporophytic divisions, MCSs following developmental types I and II were evenly stained by FDA, indicating viability of the whole structure (Fig. 4h–j, t–w). However, 2–3 days prior to exine wall rupture in MCSs following developmental type I, some domains were unstained by FDA near the area of exine wall break, opposite to the pollen germ pore (Fig. 4k, arrowhead). In the bright-field image, the FDA-unstained areas dis-

Table 1 Characterization of developmental types by time-lapse tracking of stressed barley (*Hordeum vulgare*) microspores. The development of 794 enlarged microspores was followed in three independent experiments ($n = 3$). The presence or absence of the characteristic is indicated by + or −, respectively. The percentage of star-like structures in developmental types I and II was calculated with respect to the total number of star-like structures visualized in each developmental pathway

Microspore pathways	Cells tracked	Relative frequency (%)	MCS	Gametophytic division	Cells displaying star-like structures				ELS
					Relative frequency (%) at:			Total No. at 3 days	
					0–1 days	1–2 days	2–3 days		
Type I	90	10.9 ± 4.2	+	−	65.4 ± 4.8	93.4 ± 4	100	54	+
Type II	286	36.2 ± 2.4	+	−	85.4 ± 2.5[a]	96.7 ± 2[b]	100	171	−
(I + II)	376	47.1 ± 4.5							
Type III	418	52.9 ± 4.5	−	+	−	−	−	−	−

[a]Mean value significantly different ($P < 0.06$) from value of the star-like-structure frequency in the first day of culture of developmental type I

[b]Mean value not significantly different ($P > 0.06$) from value of the star-like-structure frequency in the second day of culture of developmental type I

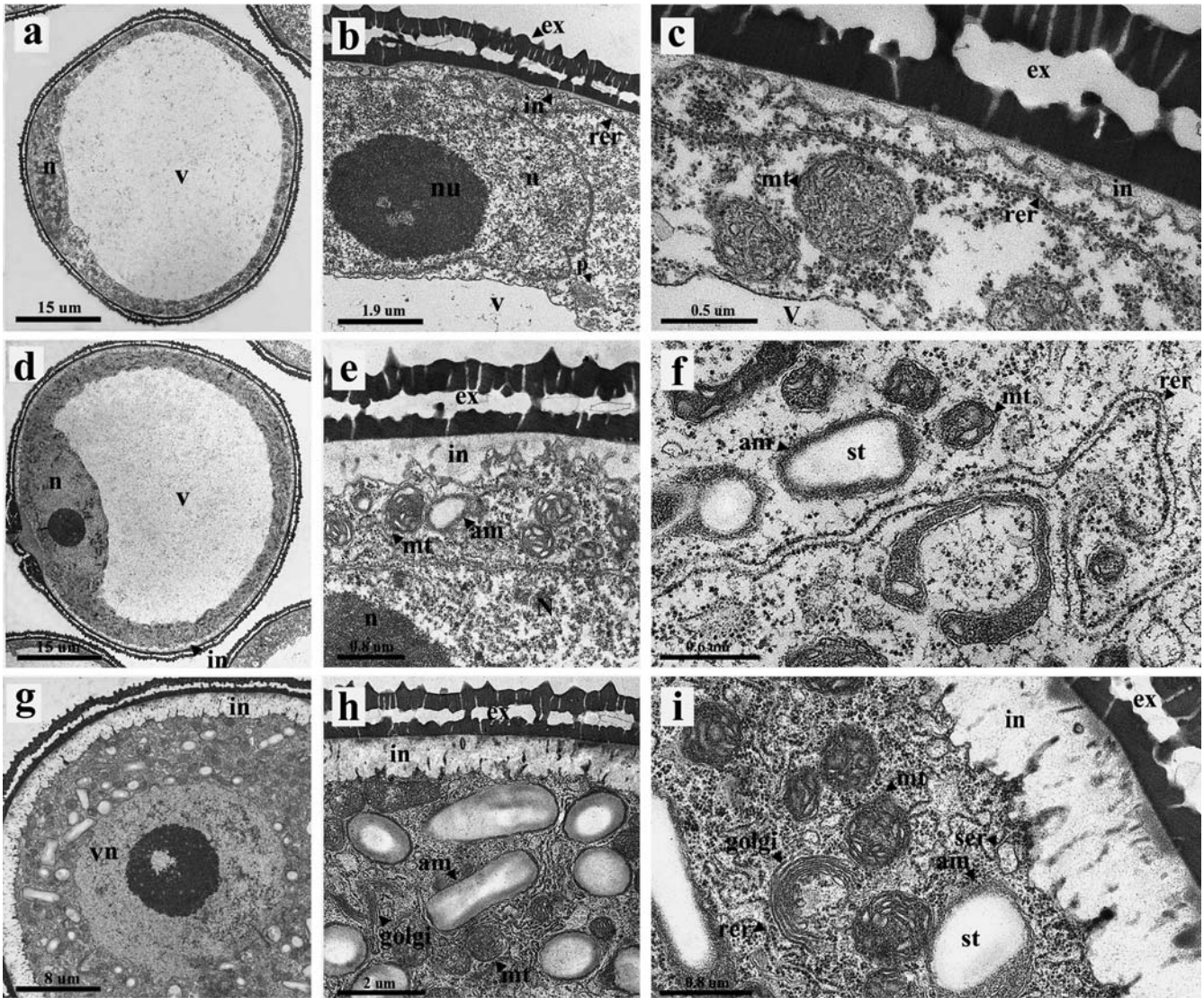

Fig. 3a–i TEM analysis of 4-day-stressed enlarged barley microspores at day 0 of culture and of binucleate pollen. **a–c** Enlarged microspores with a thin intine layer. **d–f** Enlarged microspores with a thick intine layer. **g–i** Binucleate pollen. *am* Amyloplast, *ex* exine wall, *in* intine layer, *mt* mitochondria, *nu* nucleolus, *n* nucleus, *golgi* Golgi apparatus, *p* proplastid, *rer* rough endoplasmic reticulum, *ser* smooth endoplasmic reticulum, *st* starch, *vn* vegetative nucleus

played further cell shrinkage and dead cell material was released out of the exine wall of microspores (Fig. 4e–f, l–m, arrowheads). In developmental type II, FDA-unstained domains were observed immediately prior to MCS death, about 2–4 days later than observed for MCSs following the type-I developmental pathway (Fig. 4x, arrowhead).

In order to confirm that the areas unstained by FDA represented dead cells within MCSs following the type-I developmental pathway, confocal laser scanning microscopy (CLSM) analysis of Sytox orange in combination with FDA staining was used. Sytox orange is a cell death indicator, which will only stain the nuclei of cells with damaged membranes. These studies were performed in liquid cultures of enlarged microspores due to the impossibility of using CLSM in agarose-immobilized cultures. In this system, exine wall rupture was observed after 7–8 days of culture (van Bergen et al. 1999). Therefore, FDA/Sytox orange analysis in MCSs was performed after 7 days of liquid culture. Figure 5 shows a confocal z-series of a 7-day-old MCS displaying one domain unstained by FDA, at the point of exine wall rupture (Fig. 5a,b, arrowheads). The same domain is positively stained by Sytox orange (Fig. 5c), indicating that the cells surrounding the point of exine wall break are dead.

Discussion

Morphology of microspores following androgenesis in barley

Using time-lapse tracking, mainly three developmental pathways were observed and their frequencies quantified: type I, which was the embryogenic pathway (11%);

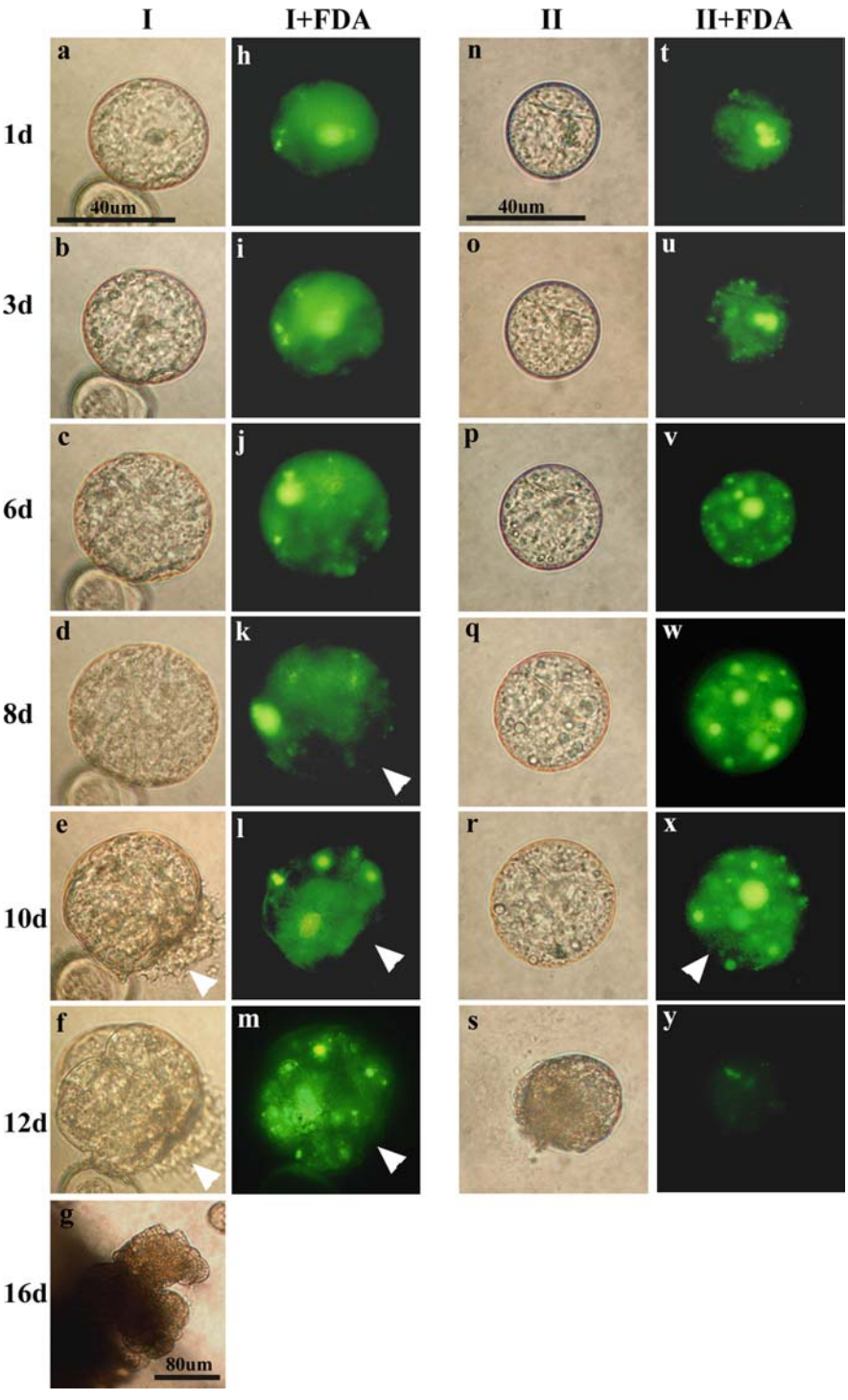

Fig. 4a–y Developmental types I (**a–m**) and II (**n–y**), as visualized by light microscopy (bright-field; columns *I* and *II*) and fluorescence microscopy after staining with FDA (columns *I + FDA* and *II + FDA*). *Arrowheads* in **e** and **f** indicate the point of exine wall rupture, and in **k–m** and **x** indicate an MCS domain with lower intensity of FDA staining. The *shadow* in **g** corresponds to the mesh used in tracking experiments

type II, which displayed sporophytic divisions, but failed to make the transition from an MCS into an ELS (36%); and type III, which degenerated in the first days of culture (53%). By tracking back these microspores to day 0 of culture, it was found that no typical morphology was associated with any of the developmental types described. Nevertheless, ultrastructural analysis of enlarged microspores by TEM revealed two distinct types of microspore. One type displayed a thin intine layer and an undifferentiated cytoplasm, while the other showed a thick intine layer and a starch-rich cytoplasm, and thus resembled developing pollen grains. Starch accumulation in the pollen amyloplasts marks the commitment to the pollen developmental pathway (McCormick 1993). Our observations indicate that the enlarged cells that evolved to pollen morphology after stress treatment were still committed to the gametophytic pathway, probably representing the developmental type III identified by time-lapse tracking. On the other hand, microspores with undifferentiated cytoplasm have been associated with the

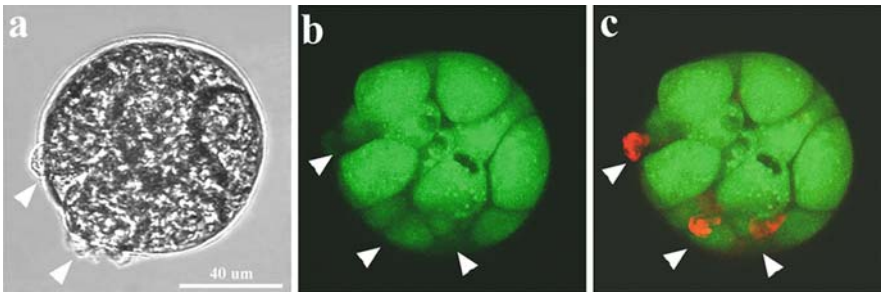

Fig. 5a–c Bright-field image (**a**) and CLSM (**b,c**) of MCSs at the stage of exine wall rupture, stained by FDA and Sytox orange. **a** Exine wall rupture in a 7-day-old MCS grown in liquid culture. The site of exine wall rupture is marked by *arrowheads*. **b** The same MCS displayed in **a** showing FDA-unstained cells at the point of exine wall rupture (*arrowheads*). **c** The FDA-unstained cells are stained by Sytox orange (*arrowheads*)

repression of the gametophytic pathway, as reported for induced tobacco, *Brassica* and wheat microspores (Rashid et al. 1982; Telmer et al. 1995; Indrianto et al. 2001). Prior to induction of androgenesis, barley uninucleate microspores are characterized by the lack of specialized morphological structures in the cytoplasm and a thin intine layer (Huang 1986). This suggests that, in barley, the microspores with undifferentiated cytoplasm and a thin intine layer after stress treatment are probably associated with the repression of the gametophytic pathway (developmental types I and II). The maintenance of a thin intine layer after stress treatment may represent an early morphological marker for induced microspores in barley.

Tracking showed that the first developmental change associated with dividing microspores (developmental types I and II) was a star-like morphology, which was characterized as a transitory stage between vacuolated microspores after stress treatment and the initiation of cell division. The occurrence of a star-like morphology appears to be correlated with embryogenic potential in other androgenic systems, such as tobacco, wheat and *Brassica* (Zaki and Dickinson 1991; Touraev et al. 1997). Though very well documented, the cellular and molecular mechanisms implicated in the central positioning of the microspore nucleus prior to its divisions are not yet clear. Increasing evidence indicates that actin filament rearrangements play a role in the division symmetry (Gervais et al. 2000) and the presence of microtubule preprophase bands was shown to be important to the symmetrical division of heat-shocked *Brassica* microspores following central localization of the nucleus (Simmonds and Keller 1999). Though the symmetry of the first division could not be verified in this study, subsequent divisions following the star-like morphology were shown to occur at the side opposite to the pollen germ pore, at the site where the generative cell is located during normal pollen development. At the stage when the dividing cells started to fill the exine cavity, they resembled very much the morphology of the cytoplasm-rich microspores previously identified by single-cell tracking as being embryogenic (Bolik and Koop 1991; Kumlehn and Lörz 1999).

Although the star-like morphology appears to be a morphological marker for the initiation of cell division in stressed microspores, a star-like morphology per se does not assure that a microspore will ultimately commit to the embryogenic pathway. According to Indrianto et al. (2001), the occurrence of a star-like morphology is a dynamic process, in which the time of occurrence will depend on the type of stress applied and the stage of microspore development. In barley, microspores of developmental type I displayed the tendency to form a star-like morphology relatively later than type-II microspores. Our results further demonstrate that the different microspore developmental pathways may reflect differences in the microspore developmental stage during the period of stress treatment.

Transition from MCSs to ELSs during androgenesis in barley

One of the main events that distinguishes androgenesis from other embryogenic systems (zygotic, somatic and apomitic) is the fact that the first divisions of induced microspores are confined by the exine wall (Mordhorst et al. 1997). Therefore, during androgenesis, embryo development relies upon rupture of the exine wall that surrounds the dividing cells. We have demonstrated that 47% of the microspores tracked were induced to divide and to form MCSs (developmental types I and II). However, only MCSs following the type-I developmental pathway were successful in making the transition from an MCS to an ELS, while MCSs from the type-II developmental pathway degenerated and died. These results indicate that successful embryo formation during androgenesis might be a two-step process. The first step would be the induction of cell divisions in those microspores that have acquired the star-like morphology after stress treatment (developmental pathways I and II). Successful ELS release out of the exine wall and further embryo formation would represent a second step that would involve the perception of other, as yet unknown, developmental cues. It is known that barley microspore embryos can progressively secrete glycosylated proteins and arabinogalactan-proteins in the course of culture, which allows the development of maize immature zygotic embryos in vitro (Paire et al. 2003). Though little is known about the mode of action of these secreted molecules in microspore embryo formation, these find-

ings indicate that stress alone does not support the embryogenic route and reinforce the idea that a second trigger might be involved. The question raised is whether developmental type II can be shifted into type I by manipulating the stress and/or culture conditions. Plant regeneration has been reported to increase as a result of application of abscisic acid during pre-treatment and by the use of ovary co-culture in low-response barley cultivars, though that seems not to be the case in the highly responsive cv. Igri (van Bergen et al. 1999; Li and Devaux 2001). In terms of breeding, it will be a challenge to determine which conditions need to be optimized in order to favor type-I development.

During androgenesis, the process of exine wall rupture has been widely accepted as a passive event that occurs by mechanical rupture due to the growing size of the dividing cells during the transition from MCSs to ELSs (Raghavan 1986). By time-lapse tracking, we have observed that exine wall rupture always occurs at the side opposite to the pollen germ pore. In wheat, exine wall rupture has been reported to occur opposite to the site of starch granule accumulation (Indrianto et al. 2001). MCSs from monocots such as barley, maize and wheat are known to possess two domains with different cellular organizations (Sunderland and Huang 1985; Huang 1986; Bonet and Omedilla 2000; Magnard et al. 2000; Ramírez et al. 2001; Testillano et al. 2002). In contrast, the divisions that take place inside the exine wall appear to be random in *Brassica* microspores and no defined site of exine wall rupture has been reported (Telmer et al. 1995; Yeung et al. 1996). The highly organized structure of microspore-derived MCSs from monocots and the reports of a defined site for exine wall rupture indicate that exine rupture might be a controlled process rather than a passive event.

Further evidence that may support this idea is the finding that the cells on the side opposite to the pollen germ pore die prior to exine wall rupture. During androgenesis, the death of specific cell types has been described within microspore-derived MCSs from many plant species. Depending on the type of developmental pathway, the vegetative or the generative nucleus divides and the undivided nucleus degenerates and dies, a process that envisages the elimination of undesired cells (Raghavan 1986). Barley MCSs are known to have diverse origins, and both vegetative and generative cell origins have been reported (Sunderland et al. 1979). Though the vegetative or generative origin of the dying cells on the side opposite to the pollen germ pore is not yet known, the side opposite to the pollen germ pore is where the generative nucleus is positioned after the first pollen mitosis during normal pollen development (Huang 1986). This suggests that this may be a position-determined cell death. Clear examples of position-determined cell death are found during xylem formation (Bhalerao and Bennett 2003) and during both female gametophyte development and fertilization. During megasporogenesis, only the chalazal-most megaspore survives while the other three undergo cell death (Drews et al. 1998), whereas during fertilization only the synergid that is located on the side close to the placenta where pollen tubes turn into the ovule degenerates (Wu and Cheung 2000). In both cases, cell death has been shown to present features of programmed cell death (PCD), a genetically regulated process that occurs upon plant development both in vivo and in vitro and responds to positional and temporal cues (Wu and Cheung 2000). Developmental uses of PCD comprise a wide range of purposes, mostly associated with shape remodelling of the plant body plan (Pennell and Lamb 1997). During in vitro somatic embryogenesis in Norway spruce (*Picea abies* L. Karst), PCD takes place during the transition phase from pro-embryogenic mass to somatic embryo (Filonova et al. 2000b) and has recently been demonstrated to be essential for correct embryo pattern formation (Bozhkov et al. 2004). In our system, successful embryogenesis relied on position-determined cell death, which preceded the release of ELSs out of the exine wall of MCSs. Our immediate aim will be to investigate whether PCD is involved in the execution of exine wall rupture and further embryogenic development during barley androgenesis.

Acknowledgements We are grateful to Sandra van Bergen (TNO Department of Applied Plant Sciences, The Netherlands) for technical assistance and valuable discussion and Dr. Wessel de Priester (Institute of Biology Leiden, Leiden University, The Netherlands) for critical reading of the manuscript.

References

Bhalerao RP, Bennett MJ (2003) The case of morphogens in plants. Nature Cell Biol 5:939–943

Bolik M, Koop HU (1991) Identification of embryogenic microspores of barley (*Hordeum vulgare* L.) by individual selection and culture and their potential for transformation by microinjection. Protoplasma 162:61–68

Bonet FJ, Olmedilla A (2000) Structural changes during early embryogenesis in wheat pollen. Protoplasma 211:94–102

Boutilier KA, Ginés MJ, DeMoor JM, Huang B, Baszczynski CL, Iyer VN, Miki BL (1994) Expression of the BnmNAP subfamily of napin genes coincides with the induction of *Brassica* microspore embryogenesis. Plant Mol Biol 26:1711–1723

Boutilier K, Offringa R, Sharma VK, Kieft H, Ouellet T, Zhang L, Hattori J, Liu CM, van Lammeren AAM, Miki BLA, Custers JBM, van Lookeren Campagne MM (2002) Ectopic expression of BABY BOOM triggers a conversion from vegetative to embryogenic growth. Plant Cell 14:1737–1749

Bozhkov PV, Filonova LH, Suarez MF, Helmersson A, Smertenko AP, Zhivotovsky, von Arnold S (2004) VEIDase is a principal caspase-like activity involved in plant programmed cell death and essential for embryonic pattern formation. Cell Death Differ 11:175–182

Drews GN, Lee D, Christensen CA (1998) Genetic analysis of female gametophyte development and function. Plant Cell 10:5–17

Filonova LH, Bozhkov PV, von Arnold S (2000a) Developmental pathway of somatic embryogenesis in *Picea abies* as revealed by time-lapse tracking. J Exp Bot 51:249–264

Filonova LH, Bozhkov PV, Brukhin VB, Daniel G, Zhivotovsky B, von Arnold S (2000b) Two waves of programmed cell death occur during formation and development of somatic embryos in the gymnosperm, Norway spruce. J Cell Sci 113:4399–4411

Gervais G, Newcomb W, Simmonds DH (2000) Rearrangement of the actin filament and microtubule cytoskeleton during induction of microspore embryogenesis in *Brassica napus* L. cv Topas. Protoplasma 213:194–202

Golds TJ, Babczinsky J, Rauscher G, Koop HU (1992) Computer-controlled tracking of single cell development in *Nicotiana tabacum* L. and *Hordeum vulgare* L. protoplasts embedded in agarose/alginate films. J Plant Physiol 140:582–587

Guha S, Maheshwari SC (1964) In vitro production of embryos from anthers of *Datura*. Nature 204:497

Hoekstra S, van Zijderveld MH, Louwerse JD, Heidekamp F, van der Mark F (1992) Anther and microspore culture of *Hordeum vulgare* L. cv. Igri. Plant Sci 86:89–96

Hoekstra S, van Zijderveld MH, Heidekamp F, van der Mark F (1993) Microspore culture of *Hordeum vulgare* L.: the influence of density and osmolarity. Plant Cell Rep 12:661–665

Huang B (1986) Ultrastructural aspects of pollen embryogenesis in *Hordeum*, *Triticum* and *Paeonia*. In: Hu H, Hongyuan Y (eds) Haploids of higher plants in vitro. Springer, Berlin Heidelberg New York, pp 91–117

Indrianto A, Barinova I, Touraev A, Heberle-Bors E (2001) Tracking individual wheat microspores in vitro: identification of embryogenic microspores and body axis formation in the embryo. Planta 212:163–174

Krens FA, Verhoeven HA, van Tunen AJ, Hall RD (1998) The use of an automated cell tracking system to identify specific cell types competent for regeneration and transformation. In vitro Cell Dev Biol Plant 34:81–86

Kumlehn J, Lörz H (1999) Monitoring sporophytic development of individual microspores of barley (*Hordeum vulgare* L.). In: Clement C, Pacini E, Audran JC (eds) Anther and pollen: from biology to biotechnology. Springer, Berlin Heidelberg New York, pp 183–189

Li H, Devaux P (2001) Enhancement of microspore culture efficiency of recalcitrant barley genotypes. Plant Cell Rep 20:475–481

Magnard JL, Le Deunff E, Domenech J, Rogowsky PM, Testillano PS, Rougier M, Risueño MC, Vergne P, Dumas C (2000) Genes normally expressed in the endosperm are expressed at early stages of microspore embryogenesis in maize. Plant Mol Biol 44:559–574

Maraschin SF, Lamers GEM, de Pater BS, Spaink HP, Wang M (2003) 14-3-3 isoforms and pattern formation during barley microspore embryogenesis. J Exp Bot 51:1033–1043

McCormick S (1993) Male gametophyte development. Plant Cell 5:1265–1275

Mordhorst AP, Toonen MAJ, de Vries SC (1997) Plant embryogenesis. Crit Rev Plant Sci 16:535–576

Paire A, Devaux P, Lafitte C, Dumas C, Matthys-Rochon E (2003) Proteins produced by barley microspores and their derived androgenic structures promote in vitro zygotic maize embryo formation. Plant Cell Tissue Org 73:167–176

Pechan PM, Smykal P (2001) Androgenesis: affecting the fate of the male gametophyte. Physiol Plant 111:1–8

Pennell RI, Lamb C (1997) Programmed cell death in plants. Plant Cell 9:1157–1168

Raghavan V (1986) Pollen embryogenesis. In: Barlow PW, Green PB, Wylie CC (eds) Embryogenesis in angiosperms. Cambridge University Press, Cambridge, pp 153–189

Ramírez C, Testillano PS, Castillo AM, Vallés MP, Coronado MJ, Cistué L, Risueño MC (2001) The early microspore embryogenesis pathway in barley is accompanied by concrete ultrastructural and expression changes. Int J Dev Biol 45:57–58

Rashid A, Siddiqui AW, Reinert J (1982) Subcellular aspects of origin and structure of pollen embryos of *Nicotiana*. Protoplasma 113:202–208

Reynolds TL (1997) Pollen embryogenesis. Plant Mol Biol 33:1–10

Simmonds DH, Keller WA (1999) Significance of preprophase bands of microtubules in the induction of microspore embryogenesis of *Brassica napus*. Planta 208:383–391

Schmidt EDL, Guzzo F, Toonen MAJ, de Vries SC (1997) A leucine-rich repeat containing receptor-like kinase marks somatic plant cells competent to form embryos. Development 124:2049–2062

Smykal PM, Pechan P (2000) Stress, as assessed by the appearance of sHsp transcipts, is required but not sufficient to initiate androgenesis. Physiol Plant 110:135–143

Somleva MN, Schmidt EDL, de Vries SC (2000) Embryogenic cells in *Dactylis glomerata* L. (Poaceae) explants identified by cell tracking and by SERK expression. Plant Cell Rep 19:718–726

Sterk P, Booij H, Schellekens GA, van Kammen A, de Vries SC (1991) Cell-specific expression of the carrot EP2 lipid transfer protein gene. Plant Cell 3:907–921

Sunderland N, Huang B (1985) Barley anther culture. The switch of programme and albinism. Hereditas 3:27–40

Sunderland N, Roberts M, Evans LJ, Wildon DC (1979) Multicellular pollen formation in cultured barley anthers. I. Independent division of the generative and vegetative cells. J Exp Bot 30:1133–1144

Telmer CA, Newcomb W, Simmonds DH (1995) Cellular changes during heat shock induction and embryo development of cultured microspores of *Brassica napus* cv. Topas. Protoplasma 185: 106–112

Testillano PS, Ramírez C, Domenech J, Coronado MJ, Vergne P, Matthys–Rochon E, Risueño MC (2002) Young microspore-derived maize embryos show two domains with defined features also present in zygotic embryogenesis. Int J Dev Biol 46:1035–1047

Toonen MAJ, Hendriks T, Schmidt EDL, Verhoeven HA, van Kammen A, de Vries SC (1994) Description of somatic-embryo-forming single cells in carrot suspension cultures employing video cell tracking. Planta 194:565–572

Touraev A, Vicente O, Heberle-Bors E (1997) Initiation of microspore embryogenesis by stress. Trends Plant Sci 2:297–302

van Bergen S, Kottenhagen MJ, van der Meulen RM, Wang M (1999) Effects of ABA during the pretreatment of barley anthers on androgenesis of *Hordeum vulgare* L. cultivars Igri and Digger. In: Clement C, Pacini E, Audran JC (eds) Anther and pollen: from biology to biotechnology. Springer, Berlin Heidelberg New York, pp 191–1999

Wang M, van Bergen S, van Duijn B (2000) Insights into a key developmental switch and its importance for efficient plant breeding. Plant Physiol 124:523–530

Yeung EC, Rahman MH, Thorpe TA (1996) Comparative development of zygotic and microspore-derived embryos in *Brassica napus* L. cv Topas. I. Histodifferentiation. Int J Plant Sci 157:27–39

Wu H, Cheung AY (2000) Programmed cell death in plant reproduction. Plant Mol Biol 44:267–281

Zaki MAM, Dickinson HG (1991) Microspore-derived embryos in *Brassica*: the significance of division symmetry in pollen mitosis I to embryogenic development. Sex Plant Rep 4:48–55